AD________________

Award Number: W81XWH-06-1-0765

TITLE: Automation and Preclinical Evaluation of a Dedicated Emission Mammotomography System for Fully 3-D Molecular Breast Imaging

PRINCIPAL INVESTIGATOR: Spencer J. Cutler

CONTRACTING ORGANIZATION: Duke University
Durham, NC 27710

REPORT DATE: October 2007

TYPE OF REPORT: Annual Summary

PREPARED FOR: U.S. Army Medical Research and Materiel Command
Fort Detrick, Maryland 21702-5012

REPORT DOCUMENTATION PAGE

Form Approved
OMB No. 0704-0188

1. REPORT DATE
01-10-2007

2. REPORT TYPE
Annual Summary

3. DATES COVERED
15 Sep 2006 – 14 Sep 2007

4. TITLE AND SUBTITLE

Automation and Preclinical Evaluation of a Dedicated Emission Mammotomography System for Fully 3-D Molecular Breast Imaging

5a. CONTRACT NUMBER

5b. GRANT NUMBER
W81XWH-06-1-0765

5c. PROGRAM ELEMENT NUMBER

6. AUTHOR(S)

Spencer J. Cutler

Email: spencer.cutler@duke.edu

5d. PROJECT NUMBER

5e. TASK NUMBER

5f. WORK UNIT NUMBER

7. PERFORMING ORGANIZATION NAME(S) AND ADDRESS(ES)

Duke University
Durham, NC 27710

8. PERFORMING ORGANIZATION REPORT NUMBER

9. SPONSORING / MONITORING AGENCY NAME(S) AND ADDRESS(ES)
U.S. Army Medical Research and Materiel Command
Fort Detrick, Maryland 21702-5012

10. SPONSOR/MONITOR'S ACRONYM(S)

11. SPONSOR/MONITOR'S REPORT NUMBER(S)

12. DISTRIBUTION / AVAILABILITY STATEMENT
Approved for Public Release; Distribution Unlimited

13. SUPPLEMENTARY NOTES

14. ABSTRACT
The overall objective of this proposal is to fully automate and optimize the performance of a 3-D dedicated emission mammotomography system for enhanced semi-automated clinical testing. A retrospective study of 103 clinical MRI uncompressed breast scans was conducted to create surface renderings of the uncompressed breasts and analyze how to adapt existing acquisition orbits for varying breast shapes. Laser ribbon ranging sensors and associated hardware to fully automate the radius of rotation were acquired and tested. An observer based 3D contrast-detail study was performed in an effort to evaluate the limits of object detectability for the dedicated CZT-based SPECT mammotomography imaging system under various imaging conditions. Other aspects of the training program were also initiated including clinical shadowing in the mammography, nuclear medicine, and breast oncology divisions at Duke University.

15. SUBJECT TERMS
Nuclear Medicine Imaging, SPECT, Molecular Breast Imaging, Mammotomography

16. SECURITY CLASSIFICATION OF:			**17. LIMITATION OF ABSTRACT**	**18. NUMBER OF PAGES**	**19a. NAME OF RESPONSIBLE PERSON**
a. REPORT	**b. ABSTRACT**	**c. THIS PAGE**			USAMRMC
U	U	U	UU	24	**19b. TELEPHONE NUMBER** *(include area code)*

Table of Contents

Introduction

The overall objective of this proposal is to fully automate and optimize the performance of a 3-D dedicated emission mammotomography system for enhanced semi-automated clinical testing. The main hypothesis of this work is that 3-D automated molecular breast imaging, with the ability to dynamically contour any sized breast, will improve detection and potentially in vivo characterization of small (<1cm) early stage breast cancer and provide a patient-flexible imaging modality ready for clinical testing. In the first year of study, 103 de-identified, retrospective clinical MRI uncompressed breast scans were obtained to create surface renderings of the uncompressed breasts and analyze how to adapt existing imaging orbits for varying breast shapes. Laser ribbon ranging sensors and associated hardware to fully automate the radius of rotation were acquired and preliminarily tested. Our first observer based 3D contrast-detail study was performed in an effort to evaluate the limits of object detectability for the dedicated CZT-based SPECT mammotomography imaging system under various imaging conditions. The molecular imaging system was also coupled onto the gantry of an x-ray computed tomography system in order to combine the benefits of both functional and anatomical hybrid imaging. Other aspects of the training program were also initiated including clinical shadowing in the mammography, nuclear medicine, and breast oncology divisions at Duke University.

Body

Task 1. Conduct a retrospective study of breast volumes, shapes, and sizes using existing anonymized bilateral MRI breast data (Refer to Appendix A for original statement of work).

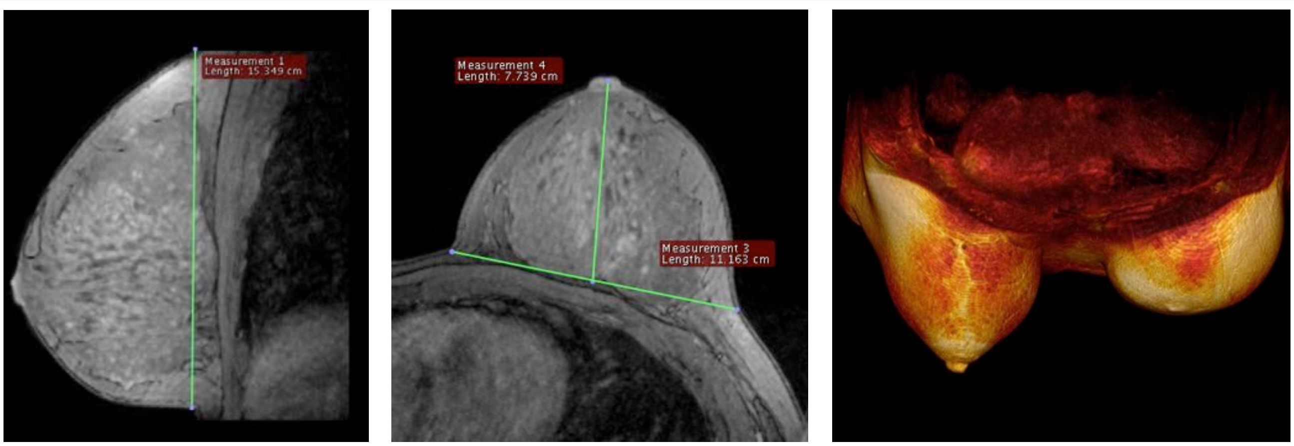

Fig. 1. Sample breast MRI sagittal (LEFT) and transverse (MIDDLE) slices with illustrated superior-inferior, nipple-chest, and medial-lateral measurements. A volumetric rendering (RIGHT) was also created for each subject.

Similar to the SPECT imaging procedure in our lab, clinical MRI images are acquired with patient lying prone, and provide a complete 3D uncompressed breast volume, useful for modeling SPECT acquisition orbits. After some delay due to schedules of three assisting physicians, my institutional review board (IRB) application was approved to obtain access to 103 unique patient MRI data sets (Appendix F). These scans were acquired previously during patients' regular visits to Duke Radiology, and represent a random sampling of high risk female breast cancer patients at the Duke University Medical Center. The volumetric data was completely de-identified except for age (Fig. 2). Breast imaging fellows provided a overview training on identifying the key landmarks of a prone breast exam.

Using open-source OsiriX imaging software, I created a database of patients and measured the pendant breast sizes: nipple-to-chest wall distance, superior-inferior distance, and medial-lateral distance (Fig 1). From the 103 subjects, a total 202 uncompressed breasts were measured (several women had complete unilateral mastectomies and therefore only the remaining breast could be measured). The initial results are tabulated in table 1 below. A 3-D surface rendering of the external breast shape was also generated in order to visualize challenges of contouring the breasts (Fig. 3) and to classify the data according to size and shape (Figs. 1,4). These MRI breast shapes can be thus used as the digital "phantoms" when utilizing computer models for system development and orbit optimization purposes (Fig. 3). Estimated volumes of the breasts are being calculated by voxel integration of the MRI images and ellipsoidal estimation given the previously measured parameters, but were not completed in time for this report.

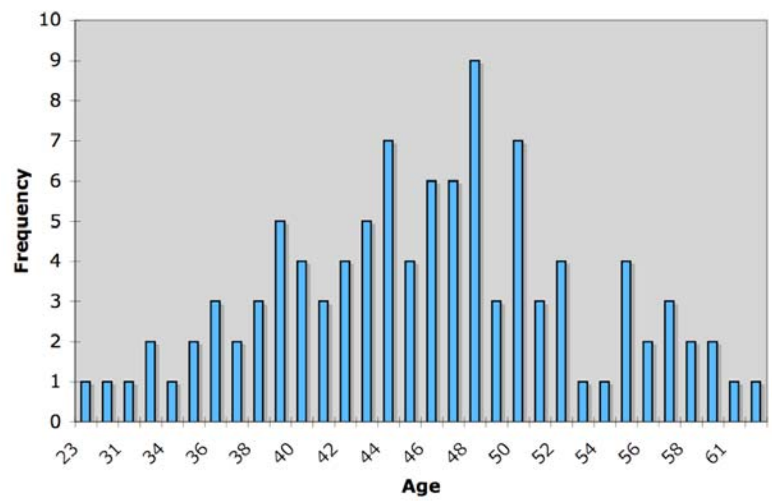

Fig. 2. Age histogram of subjects included in the MRI study.

Table 1: General statistical results for breast sizes obtained from MRI studies.

	Age (years)	Nipple-to-Chest (cm)			Medial-Lateral (cm)			Superior-Inferior (cm)		
		Right	Left	Both	Right	Left	Both	Right	Left	Both
Mean	45.8	8.0	8.4	8.2	10.5	10.6	10.5	14.2	14.1	14.1
Std. Dev.	7.6	2.5	2.9	2.7	2.4	2.5	2.4	1.7	1.5	1.6
Mode	48.0	5.5	6.9	8.4	11.5	N/A	11.5	15.2	14.9	14.9
Median	46.0	7.8	8.2	8.0	10.4	10.4	10.4	14.6	14.2	14.4
Min	23.0	3.3	2.9	2.9	5.5	6.3	5.5	8.0	8.4	8.0
Max	66.0	16.5	19.1	19.1	16.9	16.7	16.9	17.1	17.3	17.3

The study was immensely helpful in visualizing the challenging variety of breast shapes and volumes to be contoured during the SPECT scanning procedure. While the relatively low number of subjects measured prevents us from making any broad statistical classifications for the general population of women, the minimum, maximum, and mean measurements provide a starting estimate of radius-of-rotation (ROR) ranges for the gamma camera in our lab. The unique pendant breast shapes observed in this study reinforce the need to automate the ROR component of the orbit. Encouragingly, the polar tilt of our current complex orbits (Fig. 3) will sufficiently sample the majority of the shapes and volumes observed, but the ROR cannot rely on linearly interpolated points to accurately contour

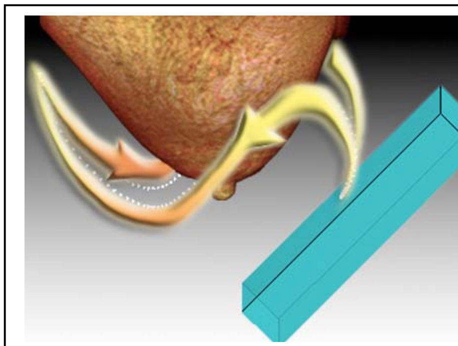
Fig. 3. (LEFT) A complex projected sine wave imaging acquisition orbit shown about a volume rendered digital breast "phantom".

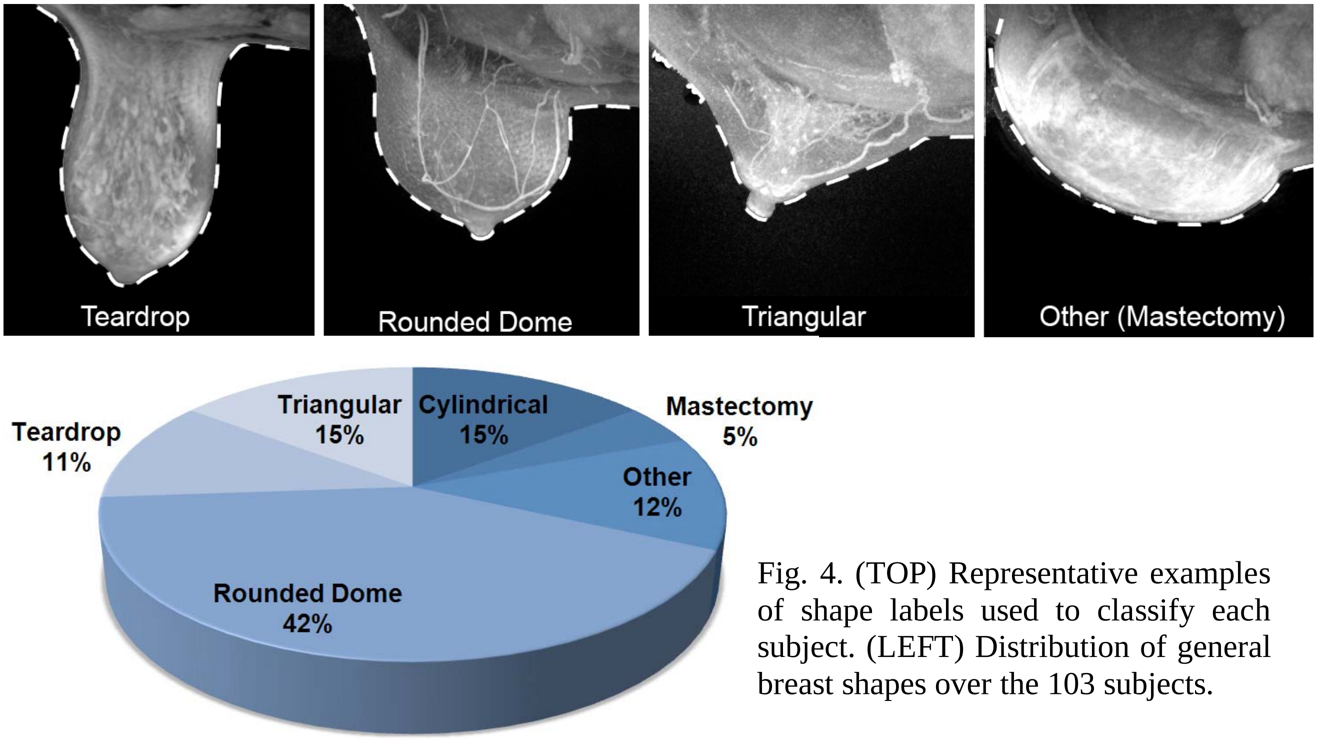

Fig. 4. (TOP) Representative examples of shape labels used to classify each subject. (LEFT) Distribution of general breast shapes over the 103 subjects.

the breast, as is currently the protocol. The measured breast sizes from this study (Fig. 4) also validate the shapes and range of sizes of the custom shaped phantoms currently used in the lab (Fig. 5).

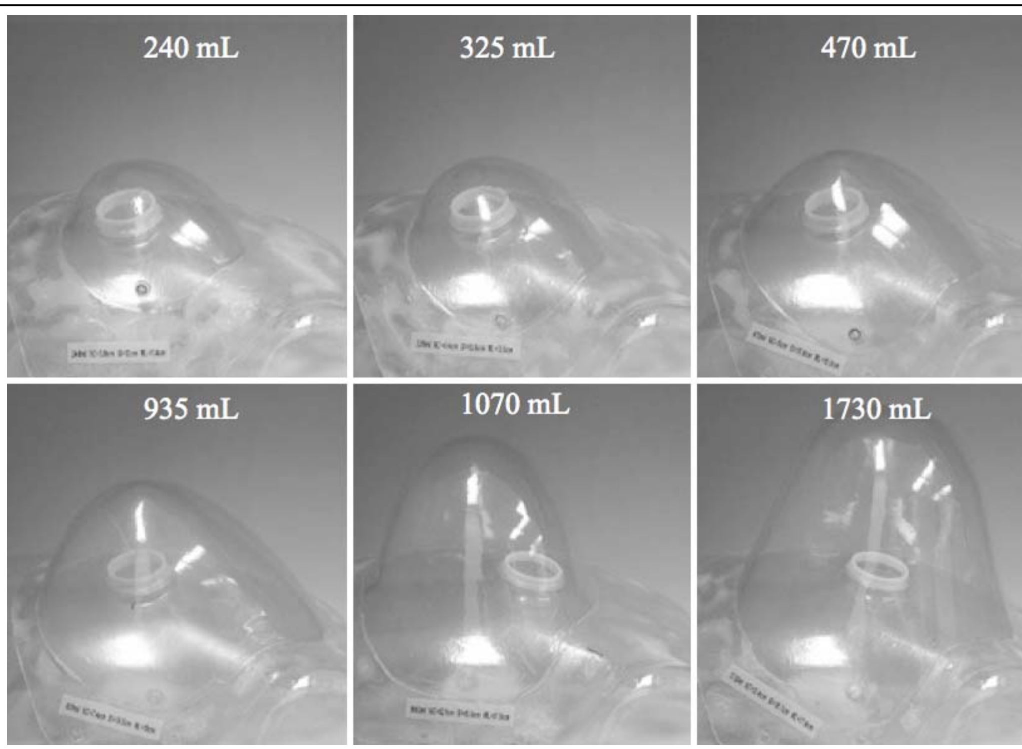

Fig. 5. Photographs of custom designed incompressible breast phantoms of varying shape and volume mounted on a chest-plate support, with truncated arm in lower right corner of each photograph.

Task 2. Implement 3-D fully automated contouring orbits for dedicated SPECT breast imaging:

Novel 3D trajectories which attempt to minimize object-detector separation, and hence optimize resolution in SPECT, have been evaluated with the system [1-3], but the manual calculation and setup for these orbits, particularly the radius-of-rotation (ROR), is time consuming and not readily adaptable to different breast shapes and sizes. A robust, fully automated solution to realize high resolution, routine human SPECT imaging given the vast array of breast shapes in healthy and diseased women is needed.

In Year 1, we have investigated reflected light, ultrasonic distance ranging, and video tracking methods, but they have poor accuracy and high divergence at close range. The proposed design uses two optical layers at known distances from the camera face, thus providing information that the breast is within some distance to the camera, but that it has/has-not penetrated the second layer (Fig. 6). Therefore, we can automate the ROR such that the breast is within ~1cm of the camera face, but not closer than 0.5cm.

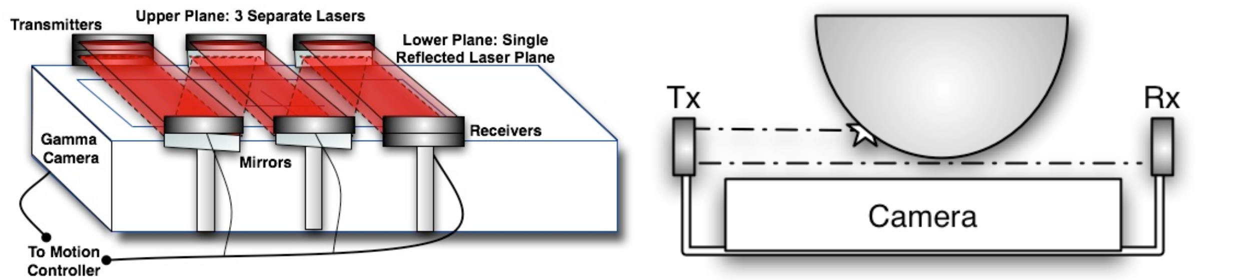

Fig. 6. (LEFT) Diagram of a dual-plane optical sensor implementation. The upper layer consists of independent, low power ribbon lasers that help identify the region on the camera face that has been penetrated, while the lower layer consists of a single, multiply reflected beam defining a virtual plane. In both layers, a receiver senses the signal intensity drop when the path of the beam is interrupted. (RIGHT) Side-view with breast penetrating upper optical sensor plane. A receiver slat may be used to distinctly separate the beams between planes.

Commercially available, low divergence, ribbon laser and optical feedback sensors (*Keyence*, 4cm wide lasers (model LV-51M) and detectors (LV-H300)) were purchased to implement this design (Fig. 7). We successfully bench tested this principle with the ribbon lasers and measured a change in beam intensity even using our clear breast phantoms (Fig. 5). I am currently working on the analog to digital conversion of the sensor outputs through the motion controller and updating the image acquisition software interface to implement the real-time feedback. 3D computer models of the sensors

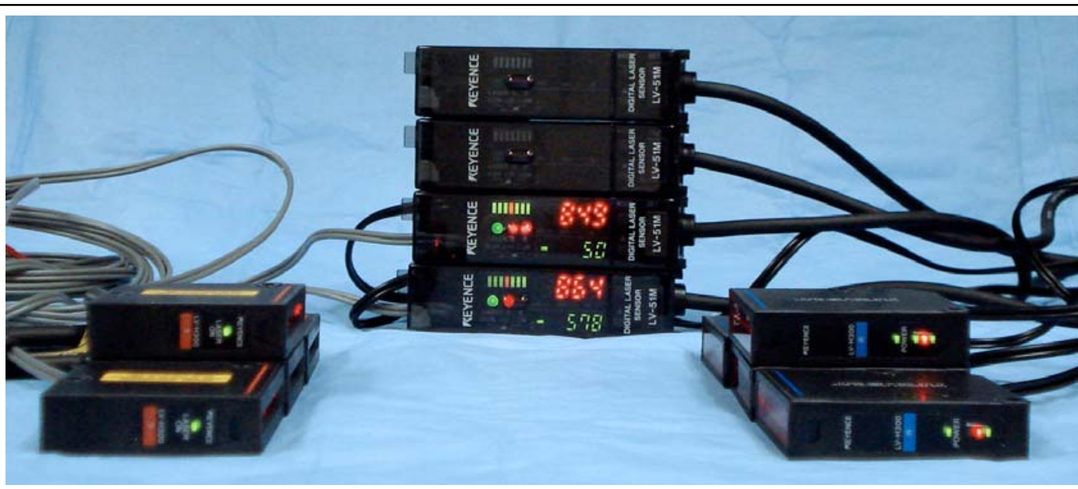

Fig. 7 Bench-top test of ribbon lasers (*Keyence).* Four 4cm wide lasers transmitters are shown at right opposite receivers at left (model LV-H300). Amplifiers with signal readout are in stacked in the middle (model LV-51M).

were also generated to experiment with various sensor configurations before investing in the appropriate mounting hardware (Fig. 8).

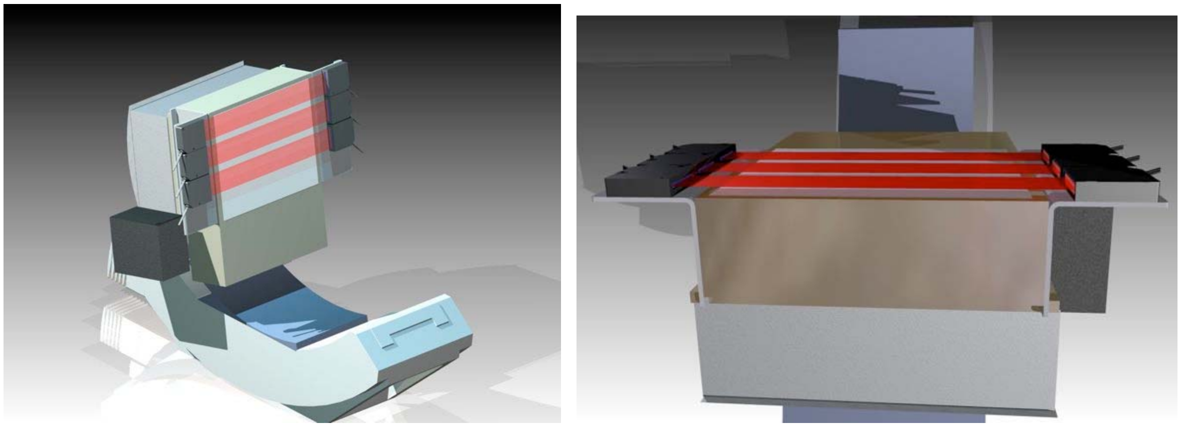

Fig. 8. (RIGHT) Computer rendered models of three ribbon laser pairs mounted on the SPECT camera's edge. (LEFT) Top-down view of a single plane of laser barriers for automated radius of rotation adjustments.

Task 3. Compare performance of the fully automated 3-D SPECT system with 2-D scintimammography:

One sub-aim of Task 3 (Appendix A) is to characterize and optimize the 3-D system using geometric phantoms. Contrast-detail observer studies are commonly used for evaluating imaging system capabilities and have been regularly used for nuclear medicine tomographic and planar imaging systems [4-6]. The goal of this study was to evaluate the minimum object size detectable under a variety of "hot and cold" signal to background contrast ratios since early and later stage, and more and less aggressive cancers take up varying amounts of tracer compounds. Since most cancerous lesions are metabolically active, imaging "hot" lesions is appropriate. Then, as cancers become more advanced, they may contain necrotic cores that do not concentrate radioactive tracers, hence "cold" imaging is also appropriate.

A novel, geometric contrast-resolution phantom was developed that can be used for both positive ("hot") and negative contrasts ("cold"). The 3cm long fillable tubes are arranged in six sectors having equal inner diameters ranging from 1mm to 6mm with plastic wall thicknesses of <0.25mm, on a pitch of twice their inner diameters (Fig. 9). Scans using simple circular trajectories were first obtained of the activity filled tubes in a uniform water filled cylinder, first with no background activity, and then varying the rod:background concentration ratios from 10:1 to 1:10. The rod phantom was then placed

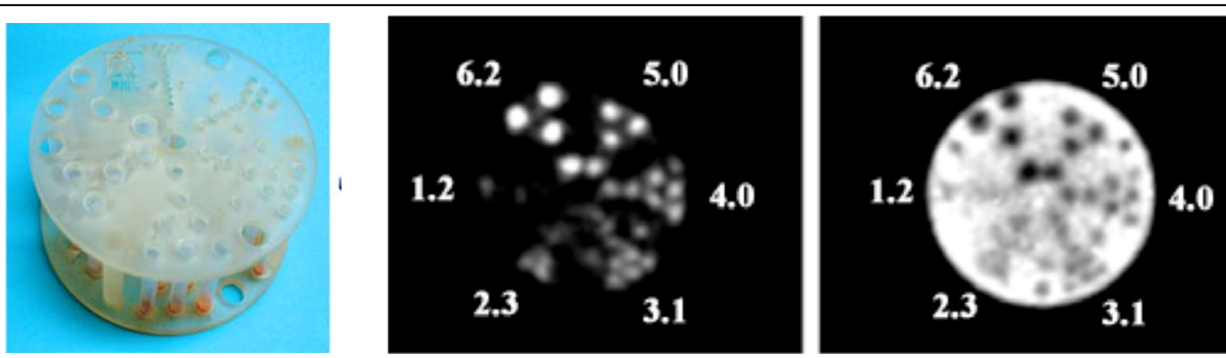

Fig. 9. (LEFT) Novel contrast-detail phantom with thin-walled PTFE tubes glued into the frame. A small amount of modeling clay (orange) was used to prevent leakage in addition to the tape used to seal the tubes. (RIGHT) Reconstructed images (5th iteration, 8 subsets, 1.25mm voxels, 15 summed slices, uniform smoothing) of phantom in cylinder for infinite:1 (Middle) and 1:10 (Right) concentration ratios. Rod sizes are indicated in mm. Note that three additional cold spots are seen (2, 6, and 10 o'clock) due to the 5mm posts holding the tube alignment layers together.

inside a non-uniformly shaped breast phantom and scans were again acquired using both simple and complex 3D trajectories for similarly varying contrasts. Scan times were adjusted to account for radioactive decay, and both low and high noise data was obtained. An iterative OSEM reconstruction algorithm was used to reconstruct the data.

Images were evaluated by six independent readers, identifying smallest distinguishable rod for each concentration and experimental setup. Results indicate that, using the SPECT camera having 2.5mm intrinsic pixels, the mean detectable size was ~3.1mm at 10:1 ratio, degrading to ~5.5mm with the 2.5:1 concentration ratio. Furthermore, there was little statistically significant difference ($p<0.05$) between cylinder vs. breast, simple vs. complex trajectories, or whether the rods appeared hot (10:1) or cold (1:10), indicating that data acquisition with the mammotomography system is quite robust. For full methods and results please refer to Appendix B.

Task 4. Complete other aspects of breast cancer training program:

In preparation for task 1, I shadowed Dr. Jay Baker, chief of the division of breast imaging at Duke University Medical Center, as he read mammograms, ultrasound, and MRI data images. The residents in the reading room were also helpful to point out the main landmarks and anatomy of MRI cross-sectional breast scans. I plan to return to the mammography clinic in the coming months to observe biopsies and mammogram imaging procedures.

To gain more clinical exposure, I also shadowed technologists in the nuclear medicine division as they injected and imaged patients (lymphoscintigraphy) prior to lymph node surgery. The technologist injects a radionuclide directly into the breast tumor and then images the patient using a large two headed gamma camera, in order to look for drainage into the lymph node. If drainage appears, the node is marked and the woman has the lymph node removed with gamma-probe guided surgery to help prevent further spreading of the cancer. I am scheduled to observe in the operation room in the coming month.

I spent my most recent round of clinical observation in the obstetrics clinic observing a new breast cancer screening approach, called random periareolar fine needle aspiration (RPFNA). RPFNA is similar to a cervical “pap-smear” in its ability to provide a representative sampling of cells from the entire breast. It has been shown to work best in women with dense breast tissue. The woman was first locally anesthetized and then eight needles per breast were used to randomly draw cells, which are later examined for abnormality. It was both sobering and motivating to observe the clinical procedures and interact with high-risk women who are clearly looking for additional diagnostic information to help them make health management decisions. Our lab hopes to collaborate in the future with the Dr. Victoria Seewaldt, who runs this Breast Wellness Center, combining our 3D molecular imaging techniques with RPFNA to provide potentially more powerful methods for breast cancer detection and diagnosis in this population of high-risk women.

Key Research Accomplishments

Year 1 included Tasks 1-2, and 4 from the original Statement of Work (Appendix A), but elements of Task 3 were also completed.

- The MRI study proposed in Task 1, analyzing 103 uncompressed breast subjects was completed. Additional volumetric calculations will be made and the database will be used to model new orbits for the system.
- Various ranging sensors were researched and laser ribbon ranging sensors were selected and acquired. 3D computer models of the sensors were also generated to simulate various sensor configurations before finalizing and fabricating the mounting hardware.

- The first observer based 3D contrast-detail study of the SPECT system was conducted and results were presented at the *2006 IEEE Nuclear Science Symposium and Medical Imaging Conference*, San Diego, CA, 29 Oct. - 4 Nov. and published in its associated conference record (Appendix B).
- Part A of Task 4 was completed, shadowing clinicians in the mammography, nuclear medicine, and breast oncology divisions at Duke University. I plan to continue participating in additional clinical experiences in the coming two years.
- The molecular SPECT imaging system was successfully coupled with an x-ray computed tomography system allowing combined functional and anatomical hybrid imaging. Results were presented at various local and international conferences (Appendices C,D).

Related:

- Additional system preclinical optimization results first authored by me for the dual-modality imaging system were accepted for an oral presentation at to the *2007 IEEE Nuclear Science Symposium and Medical Imaging Conference*, 30 October – 3 Nov., Honolulu, Hawaii. An accompanying manuscript will be submitted to the conference record.
- The first successful SPECT patient scan was conducted in the on the prototype mammotomography system in our lab with promising results (Appendix E), and we expect to complete the first subject scan with the hybrid system in the next few weeks.

Reportable Outcomes

Peer-reviewed articles

CN Brzymialkiewicz, MP Tornai, RL McKinley, **SJ Cutler**, JE Bowsher. 2006. "Performance of Dedicated Emission Mammotomography for Various Breast Shapes and Sizes." Phys. Med. Biol. 51:5051-5064.

Presentations, Published Abstracts, and Published Proceedings:

SJ Cutler, KL Perez, MP Tornai. "3-D Contrast-Detail Analysis for Dedicated Emission Mammotomography." Presented at the *2006 Nucl. Sci. Symp. & Med. Imag. Conf.*, San Diego, CA, 29 Oct. – 4 Nov. 2006, and published in *2006 IEEE Nuclear Science Symposium & Medical Imaging Conference Record*, **5**:2954 – 2958.

DJ Crotty, P Madhav, KL Perez, **SJ Cutler**, RL McKinley, T Wong, PK Marcom, MP Tornai. “3D molecular breast imaging with dedicated emission mammotomography: results of the first patient study.” Presented at the *Duke University Center for Molecular and Biomolecular Imaging Meeting*, Durham, NC, 11-13 March, 2007 and *Duke Frontiers 2007*, Durham, NC, 14 May, 2007.

P Madhav, DJ Crotty, **SJ Cutler**, KL Perez, RL McKinley, MP Tornai. “A novel dual-modality SPECT-CT system dedicated to 3D volumetric breast imaging.” Presented at the *Duke University Center for Molecular and Biomolecular Imaging Meeting*, Durham, NC, 11-13 March, 2007 and *Duke Frontiers 2007*, Durham, NC, 14 May, 2007.

MP Tornai, P Madhav, **SJ Cutler ,** DJ Crotty, RL McKinley, KL Perez, JE Bowsher. “Initial hybrid SPECT-CT system for dedicated fully-3D breast imaging.” Presented at *The Society of Nucl. Med. 54th Annual Meeting,* Washington, DC, 2-6 June 2007, and published in *J. Nucl. Med.* **48**(5). 2007.

MP Tornai, P Madhav, DJ Crotty, **SJ Cutler**, RL McKinley, KL Perez, JE Bowsher. “Application of volumetric molecular breast imaging with a dedicated SPECT-CT mammotomograph.” Presented at the *49th Annual Meeting of the American Association of Physicists in Medicine,* Minneapolis, MN, 22-26 July 2007, and published in *Med. Phys.* **34**(6):2597.

SJ Cutler, DJ Crotty, P Madhav, KL Perez, MP Tornai. “Comparison of reduced angle and fully 3D acquisition sequencing and trajectories for dual-modality mammotomography.” To be presented at the *2007 IEEE Nucl. Sci. Symposium & Med. Imaging Conference*, Honolulu, Hawaii, 28 Oct.-3 Nov. 2007

P Madhav, DJ Crotty, KL Perez, **SJ Cutler**, RL McKinley, T Wong, MP Tornai. “Initial patient study with dedicated dual-modality SPECT-CT mammotomography.” To be presented at the *2007 IEEE Nucl. Sci. Symposium & Med. Imaging Conference*, Honolulu, Hawaii, 28 Oct.-3 Nov. 2007.

Conclusions

The wide variety of breast volumes and shapes observed in 103 MRI breast subjects reinforce the need to automate the radius of rotation component of the orbit. Laser ribbon ranging sensors and associated hardware to fully automate the radius of rotation were acquired and successfully bench tested. Software and hardware system implementation are currently in progress. Results of the observer-based contrast-detail study show little statistically significant difference ($p<0.05$) between cylinder vs. breast, simple vs. complex trajectories, or whether the rods appeared hot (10:1) or cold (1:10), indicating that data acquisition with the mammotomography system is quite robust. The training program was complemented in year one with clinical shadowing experiences in multiple breast cancer related divisions of the medical center.

References

[1] CN Archer, MP Tornai, JE Bowsher, SD Metzler, BC Pieper, and RJ Jaszczak, "Implementation and initial characterization of acquisition orbits with a dedicated emission mammotomograph," *IEEE Trans. Nucl. Sci.,* vol. 50, pp. 413-420, 2003.

[2] CN Brzymialkiewicz, MP Tornai, RL McKinley, and JE Bowsher, "3D data acquisition sampling strategies for dedicated emission mammotomography for various breast sizes," *2005 IEEE Nucl Sci Symp & Med Imag Conf,* vol. 4, pp. 2596-2600, 16-22 Oct. 2004 2004.

[3] CN Brzymialkiewicz, MP Tornai, RL McKinley, SJ Cutler, and JE Bowsher, "Performance for dedicated emission mammotomography for various breast shapes and sizes," *Phys Med Biol,* vol. 51, pp. 5051-5064, 2006.

[4] K Faulkner and BM Moores, "Contrast-detail assessment of computed tomographic scanners," *Phys. Med. Biol.,* vol. 31, pp. 993-1003, 1986.

[5] DP McElroy, EJ Hoffman, L MacDonald, BE Patt, JS Iwanczyk, Y Yamaguchi, and CS Levin, "Evaluation of breast tumor detectability with two dedicated, compact scintillation cameras," *Nuclear Science, IEEE Transactions on,* vol. 49, pp. 794-802, 2002.

[6] MJ More, PJ Goodale, S Majewski, and MB Williams, "Evaluation of Gamma Cameras for Use in Dedicated Breast Imaging," *Nuclear Science, IEEE Transactions on,* vol. 53, pp. 2675-2679, 2006.

Appendices

APPENDIX A
STATEMENT OF WORK

Task 1 Conduct a retrospective study of breast volumes, shapes, and sizes using existing anonymized bilateral MRI breast data (Months 1-4):

a. Acquire IRB approval to use already acquired MRI uncompressed breast data sets for 50-100 patients (Month 1).
b. Extract the pendant breast sizes: nipple-chest wall distance, superior-inferior distance, medial-lateral distance, skin thickness, and obtain a rendering of external breast surface shape (Months 1-4).
c. Tabulate metrics of distance measurements and classify the varying spectrum of pendant breast surfaces (Month 4).

Task 2 Implement 3-D fully automated contouring orbits for dedicated SPECT breast imaging (Months 3-16):

a. Based on the results of Task 1, modify the existing basis set of orbits to account for challenges imposed by non-uniform breast shapes (Month 4).
b. Develop and implement a series of optical or ultrasonic feedback sensors on the camera for dynamic contouring. Update software interface to implement real-time feedback from sensors (Months 3-12).
c. Investigate dynamic acquisition robustness using anthropomorphic breast phantoms of varying size and shape, and compare reconstructed image quality to images acquired previously using manually defined orbits (Months 13-15).

Task 3 Compare performance of the fully automated 3-D SPECT system with 2-D scintimammography (Months 15-36):

a. Characterize and optimize 3-D system using geometric phantoms and anthropomorphic breast and torso phantoms, acquiring data under various lesion-to-background concentration conditions, with and without patient shielding, and for a variety of automated complex orbits (Months 15-21).
b. Assess reconstructed images for contrast, signal-to-noise ratio, artifacts, and lesion detectability for both low noise and clinical high noise count rates (Months 22-25).
c. Utilize compressible breast phantom containing various lesions and in varying lesion-to-background ratios to acquire 2-D planar data under varying compressions for scintimammography as well as uncompressed breast 3-D tomographic imaging (Months 26-30).
d. Conduct a limited observer study to evaluate reconstructed images for smallest lesion detectability under varying contrasts, noise levels, background uniformity, and patient shielding conditions (Months 31-36).

Task 4 Complete other aspects of breast cancer training program (Months 1-36):

a. Clinical shadowing patients having breast cancer management (Nuclear Medicine Clinic, Mammography Clinic) (Months 1-12)
b. Publish research work in peer-reviewed journals. (Months 1-36)
c. Attend and present at local Duke Medical Center lectures and medical seminars related to breast cancer (Months 1-36)
d. Attend and present work at international conferences: *DOD BCRP Era of Hope Meeting, IEEE Medical Imaging, Society of Nuclear Medicine, Radiological Society of North America,* and *San Antonio Breast Cancer Symposium*. (Months 1-36).
e. Prepare for and defend thesis (Months 30-36)

APPENDIX B

IEEE 2006 Nuclear Science Symposium and Medical Imaging Conference
Conference Record

3-D Contrast-Detail Analysis for Dedicated Emission Mammotomography

Spencer J. Cutler, *Member, IEEE*, Kristy L. Perez, *Member, IEEE*, and Martin P. Tornai, *Senior Member, IEEE*

***Abstract*– An observer based 3D contrast-detail study is performed in an effort to evaluate the limits of object detectability for a dedicated CZT-based SPECT mammotomography imaging system under various imaging conditions. A novel, geometric contrast-resolution phantom was developed that can be used for both positive ("hot") and negative contrasts ("cold"). The 3cm long fillable tubes are arranged in six sectors having equal inner diameters ranging from 1mm to 6mm with plastic wall thicknesses of <0.25mm, on a pitch of twice their inner diameters. Scans using simple circular trajectories are first obtained of the activity filled tubes in a uniform water filled cylinder, first with no background activity, and then varying the rod:background concentration ratios from 10:1 to 1:10. The rod phantom is then placed inside a non-uniformly shaped breast phantom and scans are again acquired using both simple and complex 3D trajectories for similarly varying contrasts. Scan times are adjusted to account for radioactive decay, and both low and high noise data is obtained. An iterative OSEM reconstruction algorithm is used to reconstruct the data. Images are evaluated by six independent readers, identifying smallest distinguishable rod for each concentration and experimental setup. Results indicate that, using the SPECT camera having 2.5mm intrinsic pixels, the mean detectable size was ~3.1mm at 10:1 ratio, degrading to ~5.5mm with the 2.5:1 concentration ratio. Furthermore, there was little statistically significant difference ($p<0.05$) between cylinder vs. breast, simple vs. complex trajectories, or whether the rods appeared hot (10:1) or cold (1:10), indicating that data acquisition with the mammotomography system is quite robust.**

I. Introduction

THE dedicated SPECT mammotomography imaging system in our lab allows for fully 3D imaging of a hemispherical volume about a pendant breast, and overcomes several of the physical proximity restrictions of clinical gamma cameras [1-4]. Breast imaging with clinical SPECT cameras is limited by the bulkiness of the large whole body cameras, which results in a larger radius of rotation (ROR). Spatial resolution degrades with increasing distance from the collimator in SPECT, and the larger ROR additionally results in degradation in image quality. The compact gamma camera and flexible system gantry allows close contouring of the pendant, uncompressed breast along with the ability to image lesions close to the chest wall.

With the implementation of this 3D dedicated molecular imaging system, it is necessary to evaluate and characterize system performance to provide tangible motivation for further clinical testing of this paradigm. In previous studies, lesion detectability for varying lesion sizes and contrast ratios has been evaluated using quantitative signal to noise ratio and lesion to background contrast measurements [1, 3, 5]. In order to more fully characterize the system for an object detection imaging task, an observer study is desirable.

Contrast-detail observer studies are commonly used for evaluating imaging system capabilities and have been regularly used for nuclear medicine tomographic and planar imaging systems [6-8]. The goal of this study is to evaluate the minimum object size detectable under a variety of "hot and cold" signal to background contrast ratios since early and later stage, and more and less aggressive cancers take up varying amounts of tracer compounds. Since most cancerous lesions are metabolically active, imaging "hot" lesions is appropriate. Then, as cancers become more advanced, they may contain necrotic cores which do not concentrate radioactive tracers, hence "cold" imaging is also appropriate.

II. Methods

The compact gamma camera used on our system is the CZT-based *LumaGEM*™ 3200S (*Gamma Medica*, Northridge, CA) with a measured energy resolution of 6.7% FWHM at 140 keV, a sensitivity of 37.9 cps/MBq, and $2.5 \times 2.5\text{mm}^2$ discrete pixels [3].

A. Contrast-Detail Phantom Design

A unique geometric contrast-resolution phantom was developed that can be used for both positive ("hot") and negative contrasts ("cold") (Fig. 1). The frame was digitally designed using *Autodesk Inventor* software, and then constructed using 3D stereolithography (*American Precision Prototyping*, Tulsa, OK) using a water resistant resin, DSM Somos® 11120 (density ~1.12 g/cm^3). The 3cm long thin-walled PTFE plastic tubes (*Small Parts, Inc.*, Miami Lakes, FL) of equal inner diameters (6.2, 5.0, 4.0, 3.1, 2.3, and 1.2mm with wall thicknesses of <0.25mm), on a pitch of twice their inner diameter are arranged in six sectors. For the three smallest diameter sectors, two additional tubes were added, spaced at three times their inner diameter, in order to evaluate if rods were visible at all, regardless of satisfying Nyquist's criteria. Tubes can be independently filled using equal

Manuscript received November 17, 2006. This work was funded by the National Cancer Institute of the National Institutes of Health (R01-CA096821 and EB001040), and the Department of Defense Breast Cancer Research Program (W81XWH-06-1-0765), and in part by Duke BME.

The authors are with the Multi-Modality Imaging Lab in the Department of Radiology at Duke University Medical Center, the Department of Biomedical Engineering, and the Medical Physics Graduate Program at Duke University, Durham, NC 27710, USA (email:spencer.cutler@duke.edu).

concentrations of activity and then sealed on their open ends with thin plastic tape.

Though loosely based on a mini-cold rod phantom (model ECT/DLX-MP, *Data Spectrum Corp.*, Hillsborough, NC), this phantom can be used for any combination of concentrations; both for hot and cold spot imaging while also varying the background activity and (fluid) composition. The thin wall of the tubes results in minimal scatter and partial volume sampling effects.

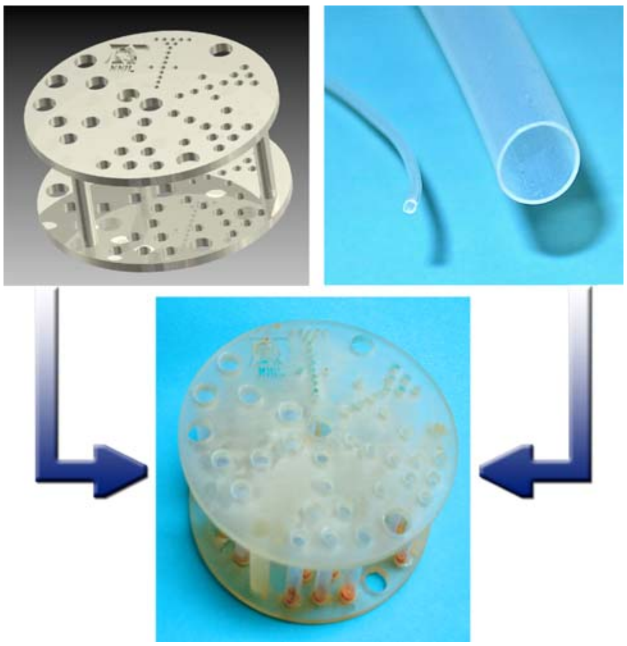

Fig. 1. (TOP LEFT) 3D rendered design of the contrast-detail phantom frame, (TOP RIGHT) Thin-walled PTFE tubing showing two different diameters, (BOTTOM) Completed contrast-detail phantom with tubes glued into the frame. A small amount of modeling clay (orange) was used to prevent leakage in addition to the tape used to seal the tubes.

B. *Rod Phantom in Uniform Cylinder*

The first set of experiments was designed to optimally image the phantom using a close ROR (4.3cm), and low scatter conditions. The phantom was placed in a uniform 7.7cm inner diameter cylinder and the background volume was filled with 215ml of water (Fig. 2).

The tubes were individually filled with aqueous [99mTc]-radioactivity with an absolute concentration of 10μCi/ml, while the background was varied, resulting in tube:background ratios of infinite:1, 10:1, 5:1, 2.5:1, 0.4:1, 0.2:1, to 0.1:1. The contrast ratios in this study are modeled

Fig. 2. Contrast-detail phantom in water filled cylinder imaged using a simple circular scan at a close radius of rotation. Blue food coloring was added to the fluid inside the tubes for better visibility.

after clinical findings that [99mTc]-sestamibi concentrates in breast tumors with a mean contrast ratio of ~5.6:1 compared to the surrounding normal tissue, varying from ~2.6:1 up to ~8.7:1 [9].

A vertical axis of rotation 360-degree circular acquisition orbit was used to acquire a total of 128 projections. Scan times were ~10 minutes and then lengthened to account for radioactive decay. Initial count rate was ~300 counts per second (cps) for the 10:1 contrast ratio, thereafter increasing proportional to the added background activity. The energy window used for this and all of the following studies was an 8% (+/- 4) window about the 140keV photopeak.

C. *Rod Phantom in Non-Uniform Breast*

The phantom was then placed inside a non-uniformly shaped breast phantom [10], giving more clinically realistic attenuation and scatter characteristics. The breast phantom was filled with 500ml of water to completely submerge the contrast-detail phantom. Scans were obtained using both a simple tilted parallel beam (TPB) and a complex projected sine wave (PROJSINE) 3D trajectory (Fig. 3, Table I). Absolute activity was again 10μCi/ml in the tubes, and activity was continually added to the background to generate the same contrast ratios as for the cylinder experiments. Scan times were again initially 10 minutes and then continually adjusted to account for radioactive decay. Initial count rate was ~480cps for the 10:1 contrast ratio.

TABLE I
PARAMETERS USED FOR BREAST EXPERIMENT ACQUISITIONS OVER A 360^o AZIMUTHAL RANGE (θ)

Orbit	Num of Prjs.	Polar Tilt, ϕ (Range, min:max)	ROR (Range, min:max [cm])
TPB	128	45^o	6.3
PROJSINE	128	15-45^o	3.3-7.6

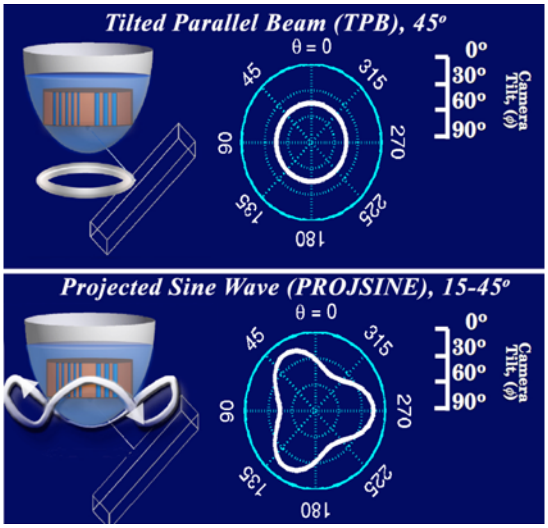

Fig. 3. Acquisition orbits, TPB and PROJSINE, used for Phantom in Breast studies. To the LEFT are visual representations of the 3D orbits and to the RIGHT are polar plots of camera tilt as a function of azimuthal angle, where the radius refers to polar tilt, and in-plane angular displacement represents azimuth.

D. High Noise Data Set

During data acquisition, noise quality inside the tubes was kept constant for each contrast ratio by adjusting the scan times for radioactive decay. The continually added activity to the background, however, results in a greater number of overall acquired counts, and therefore overall improved noise quality in the background, especially for the "cold" tube:background contrast ratios (0.4:1, 0.2:1, 0.1:1, which correspond to 1:2.5, 1:5, and 1:10, respectively). To account for this in the observer study, a separate set of "high noise" images was created by uniformly, randomly down sampling the breast projection data such that the background noise quality remained constant for each concentration ratio. The total targeted counts in each downsampled projection image were randomly determined using a Poisson distribution with a mean based on the number of counts in each corresponding 10:1 concentration ratio projection image.

E. Reconstruction and Limited Observer Study

An iterative, ray-driven implemented ordered subsets expectation maximization (OSEM) algorithm, with 8 subsets and 5 iterations was used to accurately model the 3D acquisitions and reconstruct the data. For the phantom breast images, the reconstructed volume was rotated slightly so that the tubes were vertical in the sagittal plane and therefore multiple slices could be combined to enhance image quality. Single planar images were generated for each experiment set by summing planes where rods where present (15 slices) and then smoothing the planar image using the uniform smoothing kernel in *ImageJ*. The images were also rotated clockwise so that the largest diameter rods were in the same position for both the cylinder and breast experiments, in an effort to present unbiased images in the observer study.

The resulting single slice images were evaluated in random order, in a controlled environment by six independent readers, whose task was to identify the smallest distinguishable rods (details) for all concentrations, noise levels and experimental setups and acquisitions.

III. Results

A. Rod Phantom in Uniform Cylinder

Vertical circular scans about the phantom in the small cylinder at a minimum ROR represent the best possible imaging conditions for the contrast-detail studies due to the round geometric construction of the phantom with uniform vertical tubes. The entire length of phantom is imaged as near to the camera face as possible at every angle throughout the scan.

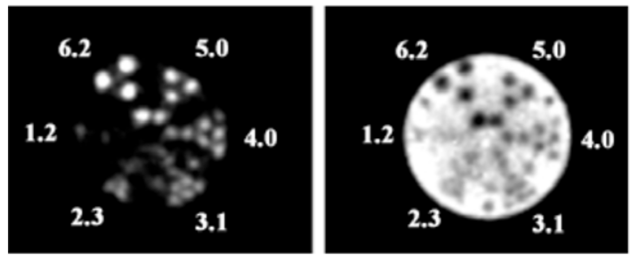

Fig. 4. Reconstructed images (5th iteration, 8 subsets, 1.25mm voxels, 15 summed slices, uniform smoothing) of phantom in cylinder for infinite:1 (LEFT) and 1:10 (RIGHT) concentration ratios. Rod sizes are indicated in mm. Note that three additional cold spots are seen (2, 6, and 10 o'clock) due to the 5mm posts holding the tube alignment layers together.

Reconstructed images from the infinite:1 (no background activity) and 1:10 rod:background concentration ratios (Fig. 4) provide a calibration reference for the other lower contrast and higher scatter and higher noise images (Fig. 5). In Fig. 4 the rods are clearly separable down to the 3.1mm sector for both the hot and cold images, as verified in the observer study results (Fig. 6). It is arguable if the 2.3mm rods are resolvable in the hot image. A small amount of activity leaked out of a few rods potentially contributing to distortion artifacts seen centrally near the 4 and 3.1 mm sectors. A partial matrix of reconstructed images of all contrasts and various acquisition setups is shown in Fig. 5.

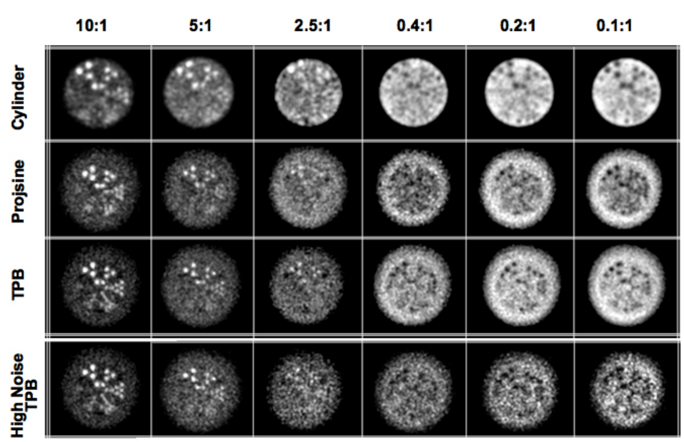

Fig. 5. Reconstructed summed slice images for concentration ratios ranging from 10:1 down to 0.1:1 (effectively 1:10) for circular scans about the cylinder, and two trajectories about the breast phantom. High noise reconstructions for the TPB orbit (only) are shown on the bottom row, where projection count densities were normalized to the 10:1 case.

Observer study results for the cylinder data demonstrate the expected trend that finer resolution is observed for higher contrasts (Fig. 6). The mean observed detail ranges from ~2.2mm in the Inf:1 case, which degrades to ~5.2mm for the 2.5:1 setup, and then inverses from ~4.4mm for the 0.4:1case improving to ~2.7mm for the 0.1:1 concentration ratio.

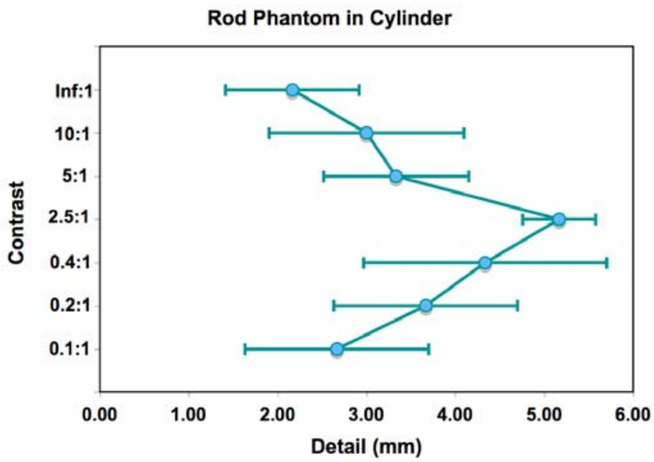

Fig. 6. Contrast vs. detail plot illustrating mean and standard deviation of independent observers.

Student t-test analysis of the cylinder results indicate that resolutions observed for positive and negative contrasts were equivalent, with no statistical differences when comparing hot vs. cold (e.g. 5:1 vs 0.2:1) for any of the contrast ratios.

B. *Rod Phantom in Non-Uniform Breast*

The increased background volume of the breast phantom creates an additional scatter medium about the rod phantom, visually apparent in the reconstructed images (Fig. 5). Although the breast phantom used is smaller than the average breast, it represents a clinically more realistic imaging subject than the cylinder.

The mean detectable rod size over all the breast acquisitions was ~3.1mm at the 10:1 concentration ratio, which degraded to ~5.9mm at the 2.5:1 concentration ratio (Figs. 7 and 8). Performance for the rod phantom in the non-uniform breast was therefore very close to that of the rod phantom in the uniform cylinder, with no significant difference at the p<0.05 level.

1) *High Vs. Low Noise Images*

Though the high noise data sets suffered from a lower number of total counts, observer detection performance remained very close to corresponding lower noise data (Figs. 7 and 8). The only statistically significant differences (p<0.05) were at the 2.5:1 concentration ratio for both TPB and PROJSINE data. At the high noise PROJSINE 2.5:1 concentration ratio, no rods were discernable by any of the readers, and thus a data point is not placed on the contrast-detail plot.

Since images are smoothed clinically before they are viewed, a modest amount of smoothing was used on all image sets. Summing multiple slices and smoothing the reconstructed images likely improved the observer results, especially for the high noise images. Though a slight separation in mean values between low and high noise data sets exists, the observer study results are promising for clinical applications where detected count densities are more similar to the high noise data.

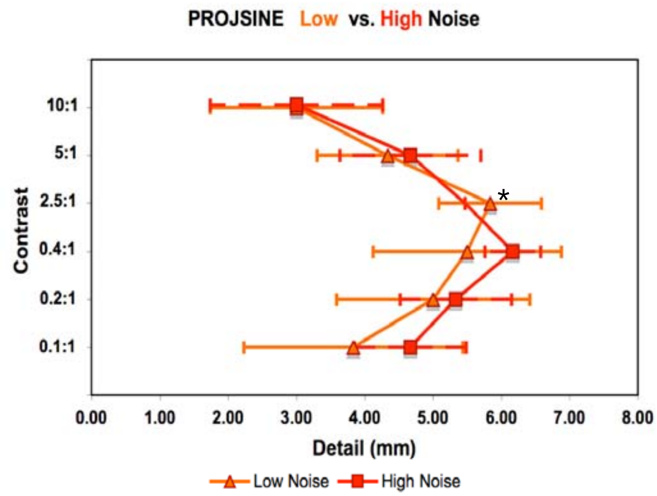

Fig. 7. Contrast vs. detail plots comparing low vs. high noise data sets for PROJSINE trajectory about the breast phantom. Asterisk denotes statistically significant differences (at p<0.05).

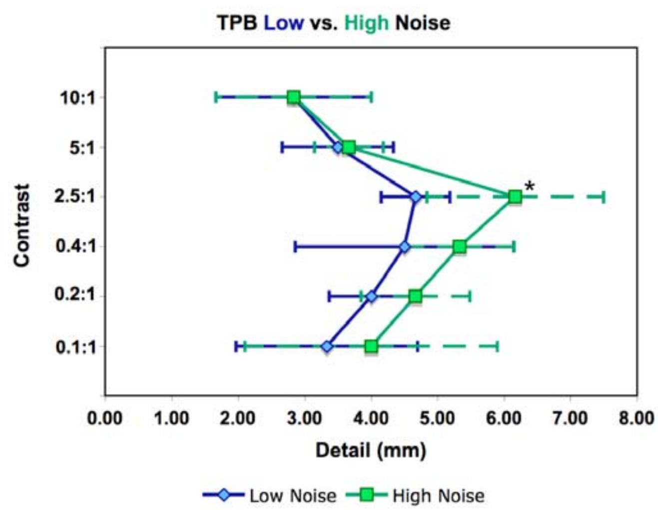

Fig. 8. Contrast vs. detail plots comparing low vs. high noise data sets for TPB orbit about the breast phantom. Asterisk denotes statistically significant differences in mean values (at p<0.05).

2) *PROJSINE vs. TPB Trajectories*

Because there was little statistical variation in detection results between the low and high noise images, the two observation sets were combined to compare performance between the two acquisition orbits (Fig 9). The TPB demonstrated significantly (p<0.05) finer resolution for the 5:1 and 2.5:1 cases. This is likely due to the fact that the TPB acquisition orbit contained many views at a closer proximity to the phantom, while PROJSINE moved farther from the rods due to variations in both polar angle and radius of rotation (Table I).

Traditional hot rod (infinite:1 contrast) and, inversely, cold rod scans were acquired using the PROJSINE orbit yielding mean observed values of ~2.4mm for Inf:1 and ~3.1mm for 1:Inf.

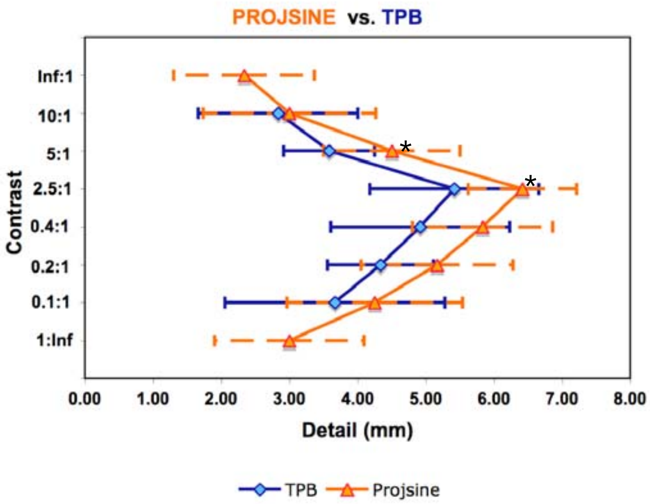

Fig. 9. Contrast vs. detail comparing PROJSINE to TPB trajectories using combined high and low noise observations. Asterisks denote statistically significant differences in mean values at p<0.05. For the Inf:1, and 1:Inf concentration ratios, only PROJSINE scans were acquired.

IV. Conclusions

A novel contrast-detail phantom was designed, constructed, and successfully used for evaluation of the dedicated emission mammography system. Results of a contrast-detail observer study indicate that, using the SPECT camera having 2.5mm intrinsic pixels, the mean detectable size over all the experiments was ~3.1mm at a 10:1 ratio, degrading to ~5.5mm with the 2.5:1 concentration ratio. Student t-tests showed little statistical significance between the higher vs. lower count densities. Resolution was proportional to the radius of rotation of the camera, highlighted for example by the observed finer resolution at 5:1 and 2.5:1 for TPB vs. Projsine scans because TPB contained more views at a closer proximity to the phantom. Furthermore, there was little statistically significant difference (p<0.05) between cylinder vs. breast, simple vs. complex trajectories, or whether the rods appeared hot (10:1) or cold (1:10), indicating that data acquisition with the mammotomography system is quite robust.

For improved accuracy, a larger sample set of images is needed to more completely characterize the system. More realistic, 3D spherical lesions should be evaluated at various contrasts for variety of breast sizes in a broader observer study, since there are advantages here of summing multiple reconstructed image planes of the symmetric rods. The developed contrast-detail phantom will, however, be useful for a variety of other applications, such as for SPECT/CT multi-modality imaging and co-registration, by placing aqueous activity in the tubes and replacing the background liquid with fluids of varying density to modify the CT contrast.

Acknowledgment

The authors thank Dominic Crotty, Randy McKinley, Priti Madhav, and Brooke Cutler for their assistance and participation in the observer study.

References

[1] C. N. Archer, M. P. Tornai, J. E. Bowsher, S. D. Metzler, B. C. Pieper, and R. J. Jaszczak, "Implementation and initial characterization of acquisition orbits with a dedicated emission mammotomograph," *IEEE Trans. Nucl. Sci.*, vol. 50, pp. 413-420, 2003.

[2] M. P. Tornai, J. E. Bowsher, C. N. Archer, J. Peter, R. J. Jaszczak, L. R. MacDonald, B. E. Patt, and J.S. Iwanczyk, "A 3D Gantry Single Photon Emission Tomograph with Hemispherical Coverage for Dedicated Breast Imaging," *Nucl. Instr. Meth. Phys. Res. A*, vol. 497, pp. 157-167, 2003.

[3] C. N. Brzymialkiewicz, M. P. Tornai, R. L. McKinley, and J. E. Bowsher, "Evaluation of Fully 3D Emission Mammotomography with a Compact Cadmium Zinc Telluride Detector," *IEEE Trans. Med. Imag.*, vol. 24, pp. 868-877, 2005.

[4] C. N. Brzymialkiewicz, M. P. Tornai, R. L. McKinley, S. J. Cutler, and J. E. Bowsher, "Performance of dedicated emission mammotomography for various breast shapes and sizes," *Physics in Medicine and Biology*, vol. 51, pp. 5051-5064, 2006.

[5] M. P. Tornai, C. N. Brzymialkiewicz, M. L. Bradshaw, J. E. Bowsher, B. E. Patt, J. S. Iwanczyk, J. Li, and L. R. MacDonald, "Comparison of compact gamma cameras with 1.3- and 2.0-mm quantized elements for dedicated emission mammotomography," *Nuclear Science, IEEE Transactions on*, vol. 52, pp. 1251-1256, 2005.

[6] K. Faulkner and B. M. Moores, "Contrast-detail assessment of computed tomographic scanners," *Phys. Med. Biol.*, vol. 31, pp. 993-1003, 1986.

[7] D. P. McElroy, E. J. Hoffman, L. MacDonald, B. E. Patt, J. S. Iwanczyk, Y. Yamaguchi, and C. S. Levin, "Evaluation of breast tumor detectability with two dedicated, compact scintillation cameras," *Nuclear Science, IEEE Transactions on*, vol. 49, pp. 794-802, 2002.

[8] M. J. More, P. J. Goodale, S. Majewski, and M. B. Williams, "Evaluation of Gamma Cameras for Use in Dedicated Breast Imaging," *Nuclear Science, IEEE Transactions on*, vol. 53, pp. 2675-2679, 2006.

[9] J. Maublant, M. de Latour, D. Mestas, A. Clemenson, S. Charrier, V. Feillel, G. Le Bouedec, P. Kaufmann, J. Dauplat, and A. Veyre, "Technetium-99m-sestamibi uptake in breast tumor and associated lymph nodes," *J Nucl Med*, vol. 37, pp. 922-5, Jun 1996.

[10] M. P. Tornai, R. L. McKinley, C. N. Bryzmialkiewicz, S. J. Cutler, and D. J. Crotty, "Anthropomorphic breast phantoms for preclinical imaging evaluation with transmission or emission imaging," in *Proc. SPIE: Phys. Med. Imag.*, San Diego, CA, USA, 2005, pp. 825-834.

APPENDIX C

Title: Initial hybrid SPECT-CT system for dedicated fully-3D breast imaging

Authors: Martin Tornai[1], Priti Madhav[1], Spencer Cutler[1], Dominic Crotty[1], Randolph McKinley[1], Kristy Perez[1], James Bowsher[2] **Institutions**: [1] Duke, Radiology & BME, Durham, NC; [2] Duke, Rad Onc, Durham, NC

Objectives: Independent SPECT and x-ray CT subsystems we developed are integrated into a single, multimodality gantry with a common FOV for uncompressed, fully-3D, inherently registered breast imaging. Resulting reconstructed whole breast and anterior chest images can be fused into a single functional-anatomical dataset for evaluation of normalcy or disease. **Methods**: The SPECT system consists of a 16x20cm^2 area CZT detector with 2.5mm pixellation and 6.7% FWHM energy resolution at 140keV (for ^{99m}Tc), and high resolution parallel hole collimator. This camera is coupled to an ROR stage, and in turn is coupled to a goniometer which can sweep the camera along a hemisphere. Combined SPECT subsystem motions allow for simple or complex trajectories along which to acquire data about a suspended, uncompressed breast. The CT subsystem consists of a tungsten x-ray target heavily K-edge filtered with Ce metal, yielding a 15% FWHM quasi-monochromatic x-ray beam at 36keV (the energy for optimal SNR^2/dose for uncompressed breast lesion imaging). The cone beam of x-rays is detected with a 20x25cm^2 CsI(Tl)-based digital x-ray detector having high efficiency for the x-rays, but considerably lower efficiency for the expected 140keV gamma rays. While both subsystems are united on a single azimuthal rotation stage, the CT system is restricted to equatorial orbits in this prototype. All data is iteratively reconstructed using OSEM for SPECT, and OSTR for CT, then registered by rigid body translations and rotations, using mixed emission/transmission external fiducial markers placed around the breast. Resulting 3D images are fused and displayed. **Results**: Initial cross contamination studies for 300-1700mL breast phantoms indicated transmission contamination of emission images was negligible (<1%), but that emission contamination of transmission images was larger, degrading reconstructed image SNR by 2030%. Use of a radio-opaque patient table reduces emission contamination considerably. Coregistered and fused data yield fine images of geometrical and anthropomorphic phantoms. **Conclusions**: The first compact hybrid SPECT-CT system dedicated to 3D breast imaging has been implemented. This versatile, volumetric system could be used for various breast diagnostics such as lesion characterization and therapeutic monitoring.

Presented at the
The Society of Nuclear Medicine 54th Annual Meeting
2-6 June, 2007
Washington, D.C.

Supporting Data:

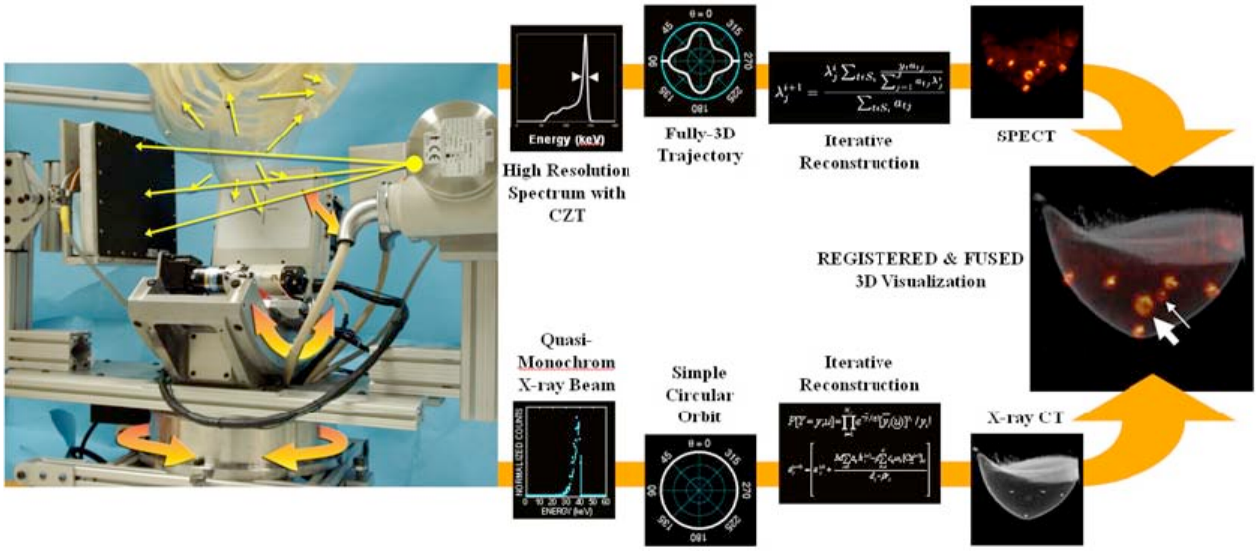

FIGURE. (Left) Photograph of the assembled hybrid imaging system along with anthropomorphic torso and breast phantoms suspended into the common field of view (FOV). Emission activity (short yellow arrows in photo) emanates from the torso and some gamma rays hit the white-faced SPECT camera, while transmission x-rays (long, directed yellow arrows in photo) travel through the breast from the x-ray tube at right to the digital detector at left. Shaded orange arrows superimposed on the positioning equipment indicate directions of motion. When combined, the SPECT system can move in fully-3D trajectories and vary its radius of rotation; the CT system is restricted to a simple circular, equatorial orbit. (From L to R on Top Orange-Flow Arrow) Cumulative 6.7% FWHM energy resolution spectrum for Tc-99m, measured with the camera; polar plot illustrating a fully-3D sinusoidal trajectory for the SPECT camera; optimizer used in the iterative reconstruction of SPECT data; colored reconstruction maximum intensity projection image (MIP) with 2.5mm voxels of an ~935mL breast phantom containing 2 activity filled balloons and 5 breast-external located fiducial markers containing small droplets of aqueous Tc-99m. (From L to R on Bottom Orange-Flow Arrow) Measured and simulated 15% FWHM quasi-monochromatic x-ray spectrum generated by heavy Ce foil K-edge filtering; polar plot illustrating the simple circular orbit for the CT camera; optimizer used in the iterative reconstruction of CT data; black-and-white reconstruction with 0.5mm voxels of MIP image of same phantom as for SPECT, after 24hr emission activity decay (air bubbles in balloons are faintly seen above the lesion volume). Note also that the fiducial markers contained iodinated contrast easily seen in the reconstructions. (Far Right) Registered and fused SPECT-CT image volume with arrows of appropriate size indicating internal lesion locations. These are more easily visualized in cine mode playback (i.e. movie) of reconstructed, registered and fused data.

APPENDIX D

A Novel Dual-Modality SPECT-CT Dedicated System for 3D Volumetric Breast Imaging

Priti Madhav, Dominic J. Crotty, Spencer J. Cutler, Randolph L. McKinley, Martin P. Tornai

Objective:
Independent dedicated SPECT and CT clinical imaging systems are integrated into a single gantry for fully-3D uncompressed breast volumetric imaging. Reconstructed images are co-registered and fused onto a single dataset to give a 3D visualization of the breast showing both functional and anatomical information that can aid in the localization and characterization of cancerous diseases.

Methods:
The SPECT (single photon emission computed tomography) system consists of a $16x20cm^2$ compound semiconductor gamma camera (6.7% FWHM at 140keV) coupled to positioning devices to permit simple and complex trajectories around a pendant uncompressed breast. The CT (computed tomography) system is comprised of a quasi-monochromatic x-ray source (~15% FWHM at 36keV mean energy) and a $20x25cm^2$ CsI(T1) digital detector having high efficiency for x-rays, but much lower efficiency for the 140keV gamma rays. With separate detectors to view the breast in the common field-of-view, the SPECT and CT systems rest on top of a common stage to allow an azimuthal rotation of 360° around the vertical breast rotation axis. The SPECT system is orthogonally juxtaposed to the cone beam x-ray source-detector axis. In contrast to the SPECT system, the CT component of the hybrid system is restricted to simple circular motions around the breast, and laterally offset from the center of rotation to prevent truncation of breasts larger than the field-of-view. Images are sequentially collected from each system and reconstructed using statistical iterative algorithms (OSEM for SPECT and OSTR for CT). Fiducial markers are localized on the external surface of the breast, facilitating post-acquisition image fusion for fully-3D functional and anatomical visualization.

Results:
Using the SPECT system, complex acquisition trajectories around the uncompressed breast allow for the detection of lesions near the axilla and chest wall, which are not visible using simple circular orbits. Due to the offset geometry, the CT system can image a wide range of breast sizes without truncation artifacts. With the use of fiducial markers, the 3D reconstructed SPECT and CT images of a water-filled breast phantom containing two water-filled balloon shaped lesions were registered together. The lesions are present for both acquisitions, but it was difficult to visualize the lesions, especially the smaller one, in the CT reconstructed images. However, with a 10:1 radioactive concentration between the lesions and background present in the SPECT images, it was considerably easier to locate both lesions.

Conclusion:
The first hybrid SPECT-CT system dedicated to 3D volumetric breast imaging has been implemented. This system offers great promise in imaging normalcy and disease in the breast: detection/staging of cancerous diseases, monitoring treatment therapies, and improving surgical biopsy guidance. Integrating both systems onto a single gantry and registering complementary anatomical and functional images is expected to help further enhance the visual and quantitative information compared with the independent systems alone.

Presented at the
Duke University Center for Molecular and Biomolecular Imaging Meeting,
Durham, NC, 11-13 March, 2007
and
Duke Frontiers 2007,
Durham, NC, 14 May, 2007

APPENDIX E

3D Molecular Breast Imaging with Dedicated Emission Mammotomography: Results of the First Patient Study

Authors: Dominic Crotty[1,2], Kristy Perez[1,2], Priti Madhav[1,2], Spencer Cutler[1,2], Randolph McKinley[1,2], Martin Tornai[1,2], Terence Wong[1,2], P. Kelly Marcom[3]

1. Department of Biomedical Engineering, Duke University, Durham NC 27708.
2. Department of Radiology, Duke University Medical Center, Durham, NC 27710.
3. Department of Oncology, Duke University Medical Center, Durham, NC 27710.

Objective: Demonstrate the imaging capability of a versatile, high performance, dedicated breast SPECT imaging system. This device could be used for diagnostic breast imaging including lesion characterization and therapeutic response monitoring using ^{99m}Tc-labeled compounds.

Methods: A patient participant with biopsy proven adenocarcinoma (T2N0), with invasive lobular and ductal features in the upper outer quadrant of the left breast was consented for the imaging study after breast MRI. 15 and 25 minutes after IV injection of 660MBq of ^{99m}Tc-sestamibi, the patient was scanned lying prone with her pendant breast suspended through a cutout on a customized, Pb-lined SPECT table. The dedicated SPECT system consists of a compact CZT gamma camera having 6.7% FWHM energy resolution and 2.5mm intrinsic spatial resolution. The camera was coupled to a positioning gantry described in detail elsewhere (*IEEE Trans. Med. Imag*. 2005,**24**(7):868) allowing fully-3D trajectories about a suspended, uncompressed breast. Image data were iteratively reconstructed with OSEM (8 subsets, 3 iterations), and smoothed with simple 3x3 boxcar kernel. Other biopsy proven participants will be similarly imaged.

Results: With dedicated SPECT, there was a clearly enhancing ~2cm diameter, detailed volume of tracer in anterior to the chest wall which corresponded to that seen in the contrast enhanced MRI scan of the same. While out of field background activity is minimized due to the use of a radio-opaque bed, streak artifacts and additional enhancing regions appear posterior to the breast, due to cardiac-hepatic uptake of tracer.

Conclusions: This compact molecular imaging system has the potential to provide quantitative 3-dimensional activity distribution information about breast cancers. It has the capability to view into the chest wall, and is not limited by breast size, density or anticipated lesion location. Since no breast compression is involved and the system has an open geometry, the patient lies comfortably on the bed, while the system non-invasively acquires tomographic image data from below. Motion artifacts were not evident with 10 minute scans. While some artifacts exist in the reconstructions, they are well understood from detailed phantom studies, and are not anticipated to detract from overall diagnostic image quality.

Presented at the
Duke University Center for Molecular and Biomolecular Imaging Meeting,
Durham, NC, 11-13 March, 2007
and
Duke Frontiers 2007,
Durham, NC, 14 May, 2007

A RETROSPECTIVE STUDY OF BREAST VOLUMES, SHAPES, AND SIZES USING EXISTING ANONYMIZED BILATERAL MRI BREAST DATA

Description of the Protocol

1. Purpose: The purpose of this study is to conduct a retrospective study of uncompressed breast volumes, shapes, and sizes using existing bilateral Magnetic Resonance Imaging (MRI) breast data at Duke. Our lab has developed a novel system for uncompressed fully three-dimensional (3D) molecular single photon emission computed tomography (SPECT) breast imaging. The compact camera and positioning hardware allow for 3D imaging anywhere about the pendant breast, providing a complete volume of image information in contrast to a single 2D, flat image. While novel 3D camera paths (orbits) have already been implemented with the system, the setup for these orbits is time consuming and not quickly adaptable to different breast shapes and sizes, and therefore is impractical for clinical imaging. The first step to automating the system is to better understand the variability in pendant, uncompressed breast shapes and sizes. A study of existing clinical MRI breast data will allow us to create surface renderings of the prone uncompressed breast and analyze how to adapt existing orbits for varying breast shapes. Additionally, having some information about the patient (weight, age, ethnicity) may prove useful in characterizing certain breast shape and volume features, as well as in organizing the database of anonymized images.

2. Background & Significance: 3D Nuclear Medicine molecular breast imaging is a promising powerful complementary imaging technique to mammography because of its ability to provide functional information about metabolic processes that can distinguish malignant and benign tissue. Our SPECT system allows for unique 3-D imaging trajectories, as opposed to simple circular orbits, with the advantage of using camera tilt to image lesions close to the chest wall as well as for axillary imaging. Currently these orbits are manually calculated. To closely contour a non-uniform uncompressed breast requires first manually moving the camera to many positions around the breast, taking measurements, and interpolating the points around the breast. A small sample of clinical, pendant MRI images of uncompressed breasts (Fig. 1) illustrate a variety of breast shapes and sizes, and reinforce the need to automate the radial (radius-of-rotation, ROR) positioning component of the orbit.

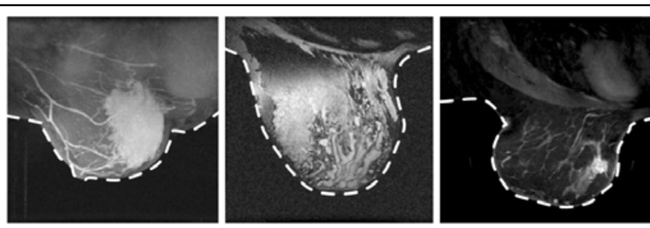

Fig. 1. Uncompressed pendant MRI images exemplify the challenges of close contouring due to varying shapes, sizes, and post-surgical abnormalities. (http://www.mrsc.ucsf.edu/breast/picts_of_breast_mri.html)

The *overall objective* of this project is to begin fully automating and optimizing the performance of the current prototype system for enhanced clinical testing. Clinical MRI images, which are also acquired with patient lying prone, are readily available and provide a complete 3D uncompressed breast volume, useful for modeling SPECT acquisition orbits. The MRI breast coil is finite in size so large breasts may have limited compression, but this should only further benefit the study as devices for breast immobilization which may have limited compression are also under investigation and development in our lab. The existing basis set of orbits will be modified to account for challenges imposed by non-uniform breast shapes. Based on the results of the study, feedback sensors will also be implemented on the camera to maintain a close proximity to the breast while avoiding contact. The result will be a highly flexible 3-D system capable of dynamically contouring breasts.

3. Design & Procedures: The Duke Advance Imaging Laboratories (Dept. Radiology) currently has over 100 volumetric breast magnetic resonance imaging data sets collected as part of another protocol (Duke University IRB # 4245). All samples are pre-existing. The images have already been removed from the clinical PACS system and de-identified prior to burning onto CD-ROMs. Patients will not be consented as the images were already collected under Duke IRB-4245. Dr. Joseph Lo of the Duke Advanced Imaging Labs will provide copies of this de-identified data with the approval of Dr. Victoria Seewaldt, PI of IRB #4245. I will not seek the identity of the participants in this study. The data will then we used to analyze pendant uncompressed breast volumes, shapes, and sizes (Fig. 1) in an effort to model ideal or "typical" orbits that may be used with patients when they would come for a SPECT scan. Duke Medical Center Breast Imaging Fellows will provide training on identifying the key landmarks of a prone breast exam. Using available OsiriX imaging software, we will read in the data and extract the pendant breast sizes: nipple-chest wall distance, superior-inferior distance, medial-lateral distance, and skin thickness. This information is useful for attenuation estimation in SPECT, and computer modeling purposes. A 3-D surface rendering of the external breast shape will also be obtained in order to visualize challenges of contouring the breasts and to classify the data according to size and shape. Fundamental metrics such as the mean and standard deviation of distance measurements will be tabulated and the varying spectrum of pendant breast surfaces can then be classified based on a variety of features (e.g. size, volume, shape). These breast shapes can then be used as the digital "phantoms" when utilizing computer models for system development and orbit optimization purposes. Metrics obtained from the image dataset may also be used in conference presentations and publications, but will not contain PHI besides those mentioned above (age at scan, pt. weight, breast cancer status or ethnicity).

4. Risk/benefit assessment:

Risks: This retrospective study represents minimal risk to the patients as the images have already been de-identified prior to being provided to the PI.

Benefits: This study will greatly benefit the lab by providing realistic digital clinical models, thereby allowing us to optimize our imaging orbits without using live patient volunteers. In the long run, it will potentially benefit volunteers and ultimately patients coming for dedicated breast SPECT scans.

5. Subject identification, recruitment, and compensation: Scans were already acquired during patients' regular visits to Duke Radiology, and represent a random sampling of high risk female breast cancer patients at the Duke University Medical Center. I will not seek to retrospectively identify or consent the participants whose image data and samples were acquired under Duke IRB 4245 and will be used in this study.

6. Subject competency: Not applicable as this is a retrospective study.

7. Costs to the subject: There are no costs to the subject involved in this study

8. Data analysis & monitoring: Images will be analyzed as outlined in Section 3, and stored in a database for future reference.

9. Data storage & confidentiality: Confidentiality will be maintained throughout this study. Data files stored at the Multi-Modality Imaging Lab will contain no private patient information. The computers are configured such that security is greater than in routinely shipped installations. Periodically, the computers are remotely scanned to determine network vulnerability or intrusion. Physical and computerized access is limited to the Duke Multi-Modality Imaging Laboratory.